JOURNAL OF PROPULSION AND POWER
Vol. 18, No. 2, March–April 2002

Dynamic Combustion of Solid Propellants: Effects of Unsteady Condensed Phase Degradation Layer

K. R. Anil Kumar* and K. N. Lakshmisha†
Indian Institute of Science, Bangalore 560012, India

A numerical model is developed for pressure- and/or radiation-driven dynamic combustion of solid propellants. The model relaxes the two key assumptions invoked in the classical, quasisteady, homogeneous, one-dimensional flame (QSHOD) model, namely, the quasisteady gas-phase (QSG) and quasisteady condensed phase degradation layer (QSC). First, the proposed non-QSC model is validated with respect to previous results of radiation-driven burning. The model is further validated for steady burning results by comparing with experimental data. Then, the effects of relaxing the QSC assumption on dynamic burning predictions are investigated under conditions of 1) an oscillating and 2) an exponentially decreasing pressure. It is confirmed that relaxing the assumptions of both QSC and QSG are equally important for computing the unsteady burning characteristics of solid propellants. For pressure-driven burning relaxing the QSC assumption results in a destabilizing effect on the frequency response function. The predicted response function magnitude is quantitatively compared with experimental data for double base propellants. The comparison seems to be better with a value of condensed phase activation energy higher than that suggested by A. A. Zenin ("Thermophysics of Stable Combustion Waves of Solid Propellants," *Nonsteady Burning and Combustion Stability of Solid Propellants*, edited by L. De Luca, E. W. Price, and M. Summerfield, Vol. 143, Progress in Astronautics and Aeronautics, AIAA, Washington, DC, pp. 197–231). Results of unsteady simulations of burning under a rapid depressurization transient exhibit salient features of combustion recovery and extinction observed in experiments. The predicted critical depressurization rate is found to markedly decrease (by a factor of four in the particular case simulated) when the QSC assumption is relaxed.

Nomenclature

A	=	preexponential factor in the Arrhenius equation for reaction rate, m, kg, s
$\mathcal{A}_c$	=	nondimensional preexponential factor in condensed phase reaction rate equation, Eq. (20)
a	=	nondimensional gas-phase heat-release parameter, Eq. (20)
c	=	specific heat, J/(kg K)
$\mathcal{D}$	=	mass diffusion coefficient in the gas phase, m^2/s
E	=	overall activation energy, J/mol
f_c	=	factor, equal to zero in QSC model and unity in non-QSC model
f_R	=	$\exp(-\kappa x_r)$, fraction of q_R absorbed below surface reaction zone
k	=	thermal conductivity, W/(m K)
Le	=	Lewis number, Eq. (20)
n	=	overall order of reaction in the gas phase
n_1	=	order of reaction in the gas phase with respect to Y_3
P	=	nondimensional pressure, Eq. (20)
p	=	pressure, Pa
Q	=	nondimensional heat release, Eq. (20)
q	=	heat release per unit reactant as a result of chemical reaction (negative for exothermic), J/kg
q_R	=	radiation heat flux incident on the interface, W/m^2
R	=	nondimensional reaction rate, Eqs. (26) and (27)
$\Re$	=	universal gas constant, 8.314 J/(mol K)
R_p	=	pressure-driven frequency response function, $(\Delta\dot{r}/\bar{\dot{r}})/(\Delta p/\bar{p})$
R_q	=	radiation-driven frequency response function, $(\Delta\dot{r}/\bar{\dot{r}})/(\Delta q_R/\bar{q}_R)$
$\dot{r}$	=	burning rate, m/s
$\dot{\boldsymbol{r}}$	=	nondimensional burning rate, Eq. (19)
T	=	temperature, K
T_b	=	$T_{-\infty} - q_g/c_g$
t	=	time, s
t_c	=	characteristic time of the condensed phase convection-conductionzone, $k_c/(\rho_c c_c \bar{\dot{r}}^2)$
t_g	=	characteristic time of the gas-phase convection-conductionzone, $k_{g,\infty}/(\rho_{g,\infty} c_{g,\infty} \bar{u}^2_{g,\infty})$
t_r	=	characteristic time of the condensed phase reaction-conductionzone, $t_c/[E_c/(2\Re\bar{T}_s)]$
u	=	velocity, m/s
W	=	molecular mass, kg/mol
$\dot{w}$	=	chemical reaction rate, Eqs. (12) and (13), $kg/(m^3 s)$
x	=	spatial coordinate, m
x_c	=	characteristic length of the condensed phase convection-conductionzone, $k_c/(\rho_c c_c \bar{\dot{r}})$
x_g	=	characteristic length of the gas-phase convection-conductionzone, $k_{g,\infty}/(\rho_{g,\infty} c_{g,\infty} \bar{u}_{g,\infty})$
x_r	=	characteristic length of the condensed phase reaction-conductionzone, $x_c/[E_c/(2\Re\bar{T}_s)]$
Y	=	mass fraction
α	=	time constant in Eq. (36)
β	=	nondimensional activation energy, Eq. (20)
γ	=	ratio of specific heats, Eq. (20)
$\delta_1, \delta_2, \delta_3$	=	defined in Eq. (20)
η	=	stretching parameter in Eq. (35)
Θ	=	nondimensional temperature, Eq. (19)
κ	=	absorption coefficient of condensed phase, m^{-1}
ν	=	frequency, Hz
ξ	=	transformed spatial coordinate, Eq. (18)
ρ	=	density, kg/m^3
τ	=	nondimensional time, Eq. (19)
χ	=	nondimensional absorption coefficient, Eq. (20)

Received 24 January 2001; revision received 6 August 2001; accepted for publication 7 August 2001.

*Research Student, Department of Aerospace Engineering; akr@aero.iisc.ernet.in.

†Assistant Professor, Department of Aerospace Engineering; knl@aero.iisc.ernet.in.

ψ = nondimensional transformed spatial coordinate, Eq. (19)

Subscripts

c = condensed phase
f = final state in a depressurization transient
g = gas phase
i = initial state in a depressurization transient
R = radiation
r = reaction zone in the condensed phase
ref = refers to conditions at $(p_{\text{ref}}, T_{-\infty})$, where p_{ref} is the mean for oscillating pressure and p_{ref} is the initial value for depressurization case
s = interface
$s+$ = interface approaching from $+\infty$
$s-$ = interface approaching from $-\infty$
0 = initial condition
1, 2, 3 = condensed phase reactant, condensed-phase product or gas-phase reactant, gas-phase product
$+\infty$ = hot boundary in the gas phase
$-\infty$ = propellant cold end

I. Introduction

In solid rocket motors the combustion zone near the propellant surface is frequently subjected to severe oscillatory or monotonic pressure changes. This often leads to highly amplified and undesirable changes in the mass burning rate. Hence the investigation of the response of the propellant burning to dynamic pressure conditions, which is usually characterized by the pressure-driven frequency response function R_p has received much attention by researchers.[1–4] A theoretical evaluation of R_p becomes difficult because of the fact that unsteady burning of solid propellants is governed by physicochemical processes in different physical phases occurring at disparate length and timescales. A schematic of such length scales around a burning surface is shown in Fig. 1. Of these, the length and timescales associated with the condensed phase thermal relaxation layer (x_c, t_c), condensed phase chemical degradation zone (x_r, t_r), and gas-phase thermal relaxation layer (x_g, t_g) are considered to be the most significant in the regime of combustion in practical motors.[5] A simplification of the problem has evolved into the classical, linear stability theory based on the quasi-steady gas- and condensed phase reaction zones, homogeneous solid, one-dimensional (QSHOD) model.[6,7] Recently, De Luca et al.[8] studied the stability under nonlinear conditions, while retaining the QSHOD assumption. This paper addresses certain issues relating to the importance of relaxing the key assumptions invoked in the QSHOD theory.

Models for dynamic combustion of solid propellants either assume region x_r (and/or x_g) as quasi-steady or neglect some of the physical/chemical processes in these regions. The QSHOD theory assumes 1) a quasi-steady gas-phase (QSG) and 2) quasi-steady condensed phase degradation zone (QSC). The bases for these assumptions[5] are, respectively, that 1) the gas-phase thermal relaxation time is much shorter than the condensed phase thermal relaxation time $(t_g \ll t_c)$ for any perturbations in external conditions such as pressure and 2) the chemical degradation layer is much thinner than the thermal diffusive layer within the propellant $(x_r \ll x_c)$. In view of the second inequality, the burning rate is assumed to follow a pyrolysis law of the Arrhenius form. The resulting R_p exhibits a peak in magnitude when the pressure fluctuations attain a frequency roughly equal to t_c^{-1}. Later studies relaxing the QSG assumption[9–13] revealed that the gas-phase unsteadiness caused by thermal inertia stabilizes the burning at low frequencies. Also, at moderately high frequencies, roughly equal to t_g^{-1}, unsteadiness of the gas phase causes significant changes with a second peak appearing in the magnitude of R_p (Refs. 9–13). However, these studies retained the QSC assumption. Consequently, the effects of relaxing the QSC assumption on the dynamic combustion characteristics are less well understood.

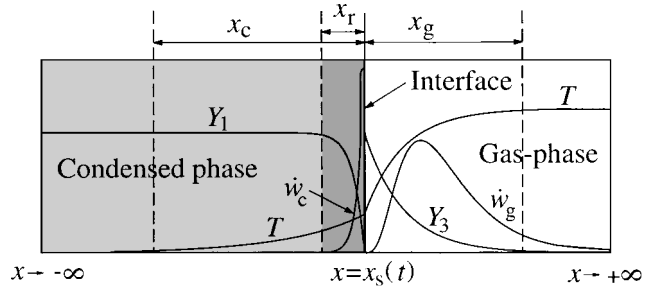

Fig. 1 Schematic of the problem domain considered. The length scales shown (not to scale) are the condensed-phase thermal layer x_c, condensed-phase degradation layer x_r, and the gas-phase thermal layer x_g. The interface is located at $x = x_s(t)$ and regresses from right to left.

An order of magnitude analysis[5] of timescales suggests that the QSC assumption might breakdown earlier (i.e., at lower frequencies) than the QSG assumption, depending upon the operating pressure and propellant properties. Low pressures and small condensed phase activation energies $(\beta_c = E_c/\Re T_b)$ are conducive to such a situation. Hence, relaxing the QSC assumption is thought to be as important as relaxing the QSG assumption, at least at frequencies near the characteristic frequency of condensed phase reaction zone t_r^{-1}. Under normal conditions $t_c > t_r > t_g$. Attempts have been made to account for the non-QSC effects by means of incorporating a distributed heat release within the condensed phase, as a uniform[8] and temperature-dependent[14] function. However, in these models the species equation in the condensed phase is not formally solved, and, hence, an ad hoc expression in the classical Arrhenius form is used to calculate the burning rate. For unsteady mass burning rate an improvement over the simple Arrhenius expression has been made by solving the species conservation equation, employing the activation energy asymptotics (AEA) technique for pressure-driven[15] and radiation-driven[16] burning in the limit of $\beta_c \to \infty$. Recently, Zebrowski and Brewster[17] examined the applicability of the large β_c limit for radiation-driven combustion by comparing the AEA results with numerical solution for finite β_c. They concluded that for realistic energetic materials the overall β_c is usually large enough so much so that a QSC description accurately predicts the steady burning rate and surface temperature. However, for unsteady burning relaxing the QSC assumption decreased the radiation-driven frequency response function R_q. Moreover, the criterion of largeness of β_c becomes more severe for dynamic burning than steady burning if QSC assumption is to be applicable. This result of Zebrowski and Brewster[17] is significant, but limited to radiation-driven burning with an adiabatic gas phase (i.e., without any heat feedback to the interface). From the practical perspective of combustion in motors, the case of pressure-driven burning including a strong, unsteady, heat feedback from the gas phase to the interface needs to be investigated.

An earlier study[18] conducted in this direction with a QSG for a double base propellant (DBP) found that a distributed heat release in the subsurface degradation layer improves the static stability, but worsens the dynamic stability when the pressure is increased suddenly. If this observation regarding dynamic stability can be (qualitatively) extended to the case of burning under a fluctuating pressure, then it would suggest that relaxing the QSC assumption should result in an increase in R_p. This would lead to a conclusion that the effect of relaxing the QSC assumption on R_p is qualitatively different from that of relaxing it on R_q. Such a conclusion appears to be important because there have been attempts to relate R_p and R_q (Ref. 19). This forms another purpose for a direct examination of the effect of relaxing the QSC assumption on R_p.

In pressure-driven burning the driving force is the fluctuation of heat feedback from the gas phase to the interface. Moreover, for the generally accepted values of gas-phase activation energy $(E_g = 5 - 15$ kcal/mol) the volumetric heat release near the interface is expected to be quite large. In such cases the fluctuations in heat feedback caused by pressure oscillations become more significant. Further, for propellants whose properties are such that $t_r/t_g = \mathcal{O}(1)$ (a likely case for AP-PBAA propellants at high pressures) unsteadiness in the condensed phase degradation layer and in the gas phase could simultaneously become important at high frequencies. Hence,

any investigation of R_p calls for a realistic gas-phase model that accurately represents these fluctuations.

Combustion of DBP is adequately represented by the one-dimensional homogeneous solid propellant model. Theoretical analyses of dynamic burning invariably invoke assumptions of overall chemical reaction and constant thermophysical properties. Generally, the exact values of these thermokinetic properties are uncertain and are often much debated. So, comparison with experimental measurements of R_p for DBP could be used to validate both the theoretical model and the set of properties of the propellants.

So far, attempts to compare theoretical predictions of R_p with experimental measurements for DBP have all used the QSHOD model.[4] Recently, within the QSHOD framework Brewster et al.[20] attempted such a comparison with the experimental data of Ibiricu.[21] Their results emphasized the importance of condensed phase reactions under dynamic burning condition. The analysis of Brewster et al.[20] showed that an improved comparison with experimental data can be obtained with a large value of E_c (=168 kJ/mol) rather than the commonly accepted value of 84 kJ/mol for many propellants, namely, N-4, N-5, and JPN. This large value of E_c was arrived at by approximating the overall condensed phase reaction by the thermal homolysis of CO-NO_2 bond, which is supposed to be the initiating step for NC/NG decomposition[22] (also, see p. 212 of Zenin[23]). However, at frequencies higher than about 3.5 kHz the response function was underpredicted; Brewster et al.[20] attributed this discrepancy to the QSC assumption.

A related situation where the burning rate undergoes large transients is when the chamber pressure monotonically changes at a rapid rate. De Luca[24] reviewed a number of studies prior to 1984 that have addressed the burning dynamics under transient external conditions. Such studies assume importance because of ignition and extinction processes. Specifically, the problem of extinction when the pressure decreases at rates faster than a critical value has been investigated both experimentally[25–28] and theoretically.[29] De Luca[24] pointed out that most of the existing theoretical studies were based on linear stability analysis. However, during a transient excursion the pressure (and hence, the surface temperature) changes involved are considerably large, and a linear analysis becomes questionable. De Luca[24] and, recently, Louwers and Gadiot[14] numerically solved the conservation equations of propellant burning subjected to a rapid depressurization. These represent studies on extinction including nonlinear effects of pressure variation. However, these retain the common QSHOD assumptions.

The main objective of this paper is to examine the effects of an unsteady degradation process within the condensed phase, on dynamic burning under conditions of a fluctuating and rapidly decreasing pressure. For this purpose a numerical model, which relaxes both the QSG and QSC assumptions, is developed to yield a fully unsteady solution of solid propellant burning. As the original conservation equations are directly solved, the results yield nonlinear stability characteristics. First, the non-QSC model is validated by comparison with the radiation-driven burning results of Zebrowski and Brewster.[17] Subsequently, the predicted steady burning results are compared with the measurements by Zenin.[23] The important differences between the QSC and non-QSC models are discussed with respect to steady burning results. The new results on dynamic burning driven by a harmonically oscillating pressure are compared with response functions measured by Ibiricu.[21] The crucial dependence of the predicted R_p on the chosen global thermokinetic properties is examined. Differences between QSC and non-QSC models are further examined with respect to the pressure-driven response function. Finally, the problem of extinction by rapid depressurization is studied. The changes in burning rate evolution, including extinction, with different depressurization rates are predicted. The effect of relaxing the QSC assumption is shown to alter significantly the predicted critical depressurization rate.

II. Description of the Physical Problem

We consider the laminar combustion of a one-dimensional solid propellant (see Fig. 1) with the following modeling assumptions:

1) The unreacted propellant is a nonporous mass of homogeneous and isotropic composition.

2) The density, thermal conductivity, and specific heat of the condensed phase are constant.

3) The condensed-phase reactant S_1 decomposes to a condensed phase product S_2 via a single-step, overall, finite rate, irreversible chemical reaction $S_1(s) \rightarrow S_2(s)$ with an overall activation energy E_c.

4) The solid-gas interface is located where the mass fraction of $S_1(s)$ reduces to zero.

5) At the interface the propellant pyrolysis and sublimation occur via the step $S_2(s) \rightarrow S_3(g)$, where S_3 is the gas-phase reactant. The interface is infinitesimally thin, planar, separating the gas phase on the right (extending to $+\infty$) from the condensed phase on the left (extending to $-\infty$).

6) The gas velocities are normal to the burning surface and are very small compared to the local acoustic velocities (low-Mach-number flow approximation).

7) The gas-phase combustion takes place via a single-step, overall, finite rate, irreversible chemical reaction $S_3(g) \rightarrow S_4(g)$, where S_4 is the gas-phase product, governed by an Arrhenius law.

8) Radiative heat transfer from the gas flame to the propellant is absent. However, the absorption of any external radiation within the condensed phase follows the Beer's law for transport of a collimated incident radiative flux in an absorbing, nonemitting, nonscattering medium with constant absorption coefficient κ.

In QSC calculations the surface pyrolysis is modeled using a more rigorous expression derived from AEA[15,19] instead of the simple Arrhenius law. Briefly, the preceding problem is a non-QSG version of Zebrowski and Brewster[17] and a non-QSC version of Anil Kumar and Lakshmisha.[13] Certain remarks regarding the assumptions for the condensed phase are in order. The spatial variation of thermophysical properties, as a result of both temperature dependence and phase transitions, is found to significantly influence the unsteady burning.[14,30] So, any further attempts to improve the present model must include 1) variable thermophysical properties and 2) a finite thickness of the phase transition zone.

III. Governing Equations

A. Conservation Equations

With the preceding assumptions the differential equations governing the unsteady burning of a solid propellant, in the laboratory-fixed coordinate system (with the origin being located arbitrarily at the initial position of the interface), take the following form:

Condensed phase species:

$$\rho_c \frac{\partial Y_1}{\partial t} = \dot{w}_c \tag{1}$$

Condensed phase energy:

$$\rho_c c_c \frac{\partial T}{\partial t} = k_c \frac{\partial^2 T}{\partial x^2} + f_c q_c \dot{w}_c + f_R q_R \kappa \exp[\kappa (x - x_s)] \tag{2}$$

In Eq. (1) species mass diffusion is neglected, as is customary. In Eq. (2) $f_c = 0$, and $f_R = \exp(-\kappa x_r)$ for QSC model and $f_c = f_R = 1$ for non-QSC model. The surface reaction assumption in the QSC model eliminates the need for solving the condensed phase species equation (1). Further, the mass fraction Y_1 becomes a step function, with $Y_1 = 1$ in the condensed phase ($-\infty \le x < x_s$) and $Y_1 = 0$ at the interface. The convective terms do not appear in Eqs. (1) and (2) as the solid is at rest relative to the coordinate system chosen.

Gas-phase continuity:

$$\frac{\partial \rho_g}{\partial t} + \frac{\partial (\rho_g u_g)}{\partial x} = 0 \tag{3}$$

Gas-phase species:

$$\rho_g \frac{\partial Y_3}{\partial t} + \rho_g u_g \frac{\partial Y_3}{\partial x} = \frac{\partial}{\partial x}\left(\mathcal{D} \rho_g \frac{\partial Y_3}{\partial x}\right) + \dot{w}_g \tag{4}$$

Gas-phase energy:

$$\rho_g c_g \frac{\partial T}{\partial t} + \rho_g u_g c_g \frac{\partial T}{\partial x} = \frac{\partial}{\partial x}\left(k_g \frac{\partial T}{\partial x}\right) + q_g \dot{w}_g + \frac{\mathrm{d}p}{\mathrm{d}t} \tag{5}$$

B. Interface Flux Balance

Overall mass:

$$\rho_c \dot{r} = \rho_g (u_g + \dot{r}) \tag{6}$$

Species:

$$(\rho_c \dot{r} Y_2)_{x_{s-},t} = [\rho_g (u_g + \dot{r}) Y_3]_{x_{s+},t} - \left(\mathcal{D} \rho_g \frac{\partial Y_3}{\partial x} \right)_{x_{s+},t} \tag{7}$$

Energy:

$$\left(k_c \frac{\partial T}{\partial x} \right)_{x_{s-},t} = \left(k_g \frac{\partial T}{\partial x} \right)_{x_{s+},t} - \rho_c \dot{r} q_s - (1 - f_c) \rho_c \dot{r} q_c + (1 - f_R) q_R \tag{8}$$

In Eqs. (6–8) the mass burning rate $\dot{r}(t)$, the gas-side species mass fraction $Y_3(x_{s+}, t)$, and the interface temperature $T_s(t)$ are unknowns and are part of the solution.

C. Initial and Boundary Conditions

$$T(x, 0) = T_0(x), \qquad Y_3(x, 0) = Y_{3,0}(x), \qquad Y_1(x, 0) = Y_{1,0}(x) \tag{9}$$

$$\left(\frac{\partial Y_3}{\partial x} \right)_{\infty,t} = 0, \qquad Y_2(x_{s-}, t) = 1 \tag{10}$$

The temperature boundary condition at the hot end is derived assuming an isentropic flow beyond the edge of the flame, as given by T'ien[9]:

$$\rho_g c_g \left(\frac{\mathrm{D}T}{\mathrm{D}t} \right)_{\infty,t} = \frac{\mathrm{d}p}{\mathrm{d}t} \tag{11}$$

D. Chemical Reaction Rates

The rate of decomposition of solid propellant is assumed to be distributed in space, but zeroth order in species Y_1. Then,

Condensed phase chemical reaction rate:

$$\dot{w}_c = -\rho_c A_c \exp(-E_c / \Re T) \tag{12}$$

whereas the distributed rate of chemical reaction within the gas-phase is modeled as follows:

Gas-phase chemical reaction rate:

$$\dot{w}_g = -A_g \rho_g^n Y_3^{n_1} \exp(-E_g / \Re T) \tag{13}$$

E. Instantaneous Burning Rate $\dot{r}(t)$ for Non-QSC Model

In a coordinate system with the origin fixed to the burning surface (x', t), the condensed-phase species conservation equation is of the form

$$\rho_c \frac{\partial Y_1}{\partial t} + \rho_c \dot{r} \frac{\partial Y_1}{\partial x'} = \dot{w}_c, \qquad Y_1(-\infty, t) = 1 \tag{14}$$

Then, assuming $Y_1(x' = 0, t) = 0$, the unsteady burning rate is given by integration of Eq. (14):

$$\dot{r}(t) = A_c \int_{-\infty}^{0} \exp\left(-\frac{E_c}{\Re T} \right) \mathrm{d}x' + \int_{-\infty}^{0} \frac{\partial Y_1}{\partial t} \mathrm{d}x' \tag{15}$$

In accordance with this, $\dot{r}(t)$ is calculated using the expression

$$\dot{r}(t) = \left| \frac{\mathrm{d}x_s}{\mathrm{d}t} \right| \tag{16}$$

where instantaneous location of the interface $x_s(t)$ is determined by the position where Y_1 reduces to zero in the condensed phase. Thus, the problem of evaluating $\dot{r}(t)$ amounts to identifying the instantaneous position of the solid-gas interface $x_s(t)$.

F. Instantaneous Burning Rate $\dot{r}(t)$ for QSC Model

The simplest way of calculating the burning rate is to assume the Arrhenius expression $\dot{r}(t) = A_s \exp(-E_s / \Re T_s)$. However, by employing AEA Lengellé[15] obtained the formal solution for the unsteady burning rate. Subsequently, Ibiricu and Williams[16] extended the analysis for radiation-driven burning:

$$\dot{r}^2 = \frac{A_c \Re T_s^2 k_c \exp[-E_c / (\Re T_s)]}{\rho_c E_c [c_c (T_s - T_{-\infty}) + q_c / 2 - f_R q_R / (\rho_c \dot{r})]} \tag{17}$$

IV. Transformation and Nondimensionalization of Equations

We apply the Lagrangian mass-weighted (von Mises') coordinate transformation[13]

$$\xi = \int_{-\infty}^{x} \rho \, \mathrm{d}x, \qquad t = t \tag{18}$$

and the transformed equations are nondimensionalized by defining the variables

$$\Theta = \frac{T - T_{-\infty}}{T_b - T_{-\infty}}, \qquad \psi = \frac{\xi}{k_{g,\mathrm{ref}} / c_g u_{\mathrm{ref}}}$$

$$\tau = \frac{t}{k_{g,\mathrm{ref}} / \rho_{g,\mathrm{ref}} u_{\mathrm{ref}}^2 c_g}, \qquad \dot{\boldsymbol{r}} = \frac{\rho_c \dot{r}}{\rho_{g,\mathrm{ref}} u_{\mathrm{ref}}} \tag{19}$$

and the parameters

$$Le = \frac{k_g}{\mathcal{D} \rho_g c_g}, \qquad \delta_1 = \frac{\rho_c k_c / c_c}{\rho_g k_g / c_g}, \qquad \delta_2 = \frac{\rho_c k_c}{\rho_g k_g}, \qquad \delta_3 = \frac{\rho_{g,\mathrm{ref}}}{\rho_c}$$

$$\gamma = 1 + \frac{\Re}{W_g c_g}, \qquad P = \frac{p}{p_{\mathrm{ref}}}, \qquad \mathcal{A}_c = A_c t_{\mathrm{ref}}, \qquad \beta_c = \frac{E_c}{\Re T_b}$$

$$\beta_g = \frac{E_g (T_b - T_{-\infty})}{\Re T_b^2}, \qquad \chi = \frac{\kappa k_{g,\mathrm{ref}}}{\rho_c c_g u_{\mathrm{ref}}}, \qquad a = \frac{T_b - T_{-\infty}}{T_b}$$

$$Q_c = \frac{q_c}{c_g (T_b - T_{-\infty})}, \qquad Q_R = \frac{q_R}{\rho_{g,\mathrm{ref}} c_c u_{\mathrm{ref}} (T_b - T_{-\infty})}$$

$$Q_s = \frac{q_s}{c_g (T_b - T_{-\infty})} \tag{20}$$

where

$$u_{\mathrm{ref}} = \left[\frac{2 A_g k_{g,\mathrm{ref}} Le^{n_1} (\rho_{g,\mathrm{ref}} T_{-\infty} / T_b)^{n-1}}{\rho_{g,\mathrm{ref}} c_g} \right]^{\frac{1}{2}} \times \left(\frac{\Re T_b^2}{E_g [T_b - T_{-\infty}]} \right)^{(n_1+1)/2} I^{\frac{1}{2}} \exp\left(-\frac{E_g}{2 \Re T_b} \right) \tag{21}$$

where

$$I = \int_0^{\infty} \left(1 + \frac{a}{\beta_g} \vartheta \right)^{n-1} \vartheta^{n_1} \exp(-\vartheta) \, \mathrm{d}\vartheta$$

For $n_1 = 1$ Williams[31] has shown that the steady-state burning rate of a solid propellant has form of Eq. (21) in the limit of $(\beta_g \to \infty, q_s \to 0)$. Therefore, Eq. (21) serves as a suitable scaling factor for the surface burning rate. Note that δ_1 is the ratio of timescales of response of the condensed phase to that of the gas phase. In the QSHOD limit $\delta_1 \to \infty$. The governing equations in the nondimensional transformed coordinates are as follows:

Condensed phase species:

$$\frac{\partial Y_1}{\partial \tau} = \dot{R}_c \tag{22}$$

Condensed phase energy:

$$\frac{\partial \Theta}{\partial \tau} = \delta_1 \frac{\partial^2 \Theta}{\partial \psi^2} + f_c Q_c \dot{R}_c + f_R Q_R \chi \exp[\chi(\psi - \psi_s)] \tag{23}$$

Gas-phase species:

$$\frac{\partial Y_3}{\partial \tau} = \frac{P}{Le} \frac{\partial^2 Y_3}{\partial \psi^2} + \dot{R}_g \tag{24}$$

Gas-phase energy:

$$\frac{\partial \Theta}{\partial \tau} = P \frac{\partial^2 \Theta}{\partial \psi^2} + \frac{\gamma - 1}{\gamma} \left(\frac{1}{a} - 1 + \Theta \right) \frac{1}{P} \frac{\mathrm{d}P}{\mathrm{d}\tau} - \dot{R}_g \tag{25}$$

Condensed phase chemical source term:

$$\dot{R}_c(\Theta) = -\mathcal{A}_c \exp\left(\frac{-\beta_c}{1 - a + a\Theta} \right) \tag{26}$$

Gas-phase chemical source term:

$$\dot{R}_g(Y_3, \Theta) = -\frac{\beta_g^{n_1 + 1}}{2Le^{n_1} I} (1 - a + a\Theta)^{1-n} P^{n-1} Y_3^{n_1} \times \exp\left[\frac{-\beta_g (1 - \Theta)}{1 - a(1 - \Theta)} \right] \tag{27}$$

The interface conditions are as follows:

Species:

$$1 = Y_3(\psi_{s+}, \tau) + \frac{P}{\dot{r} Le} \left[1 + \frac{\delta_3 (1 - a)}{1 - a + a\Theta_s} \right]^{-1} \left(\frac{\partial Y_3}{\partial \psi} \right)_{\psi_{s+}, \tau} \tag{28}$$

Energy:

$$\delta_2 \left(\frac{\partial \Theta}{\partial \psi} \right)_{\psi_{s-}, \tau} = P \left(\frac{\partial \Theta}{\partial \psi} \right)_{\psi_{s+}, \tau} - \dot{r} Q_s - (1 - f_c) \dot{r} Q_c + (1 - f_R) Q_R \tag{29}$$

Initial and boundary conditions:

$$\Theta(\psi, 0) = \Theta_0(\psi), \qquad Y_3(\psi, 0) = Y_{3,0}(\psi)$$

$$Y_1(\psi, 0) = Y_{1,0}(\psi) \tag{30}$$

$$\left(\frac{\partial Y_3}{\partial \psi} \right)_{\infty, \tau} = \Theta(0, \tau) = Y_3(\psi_{s-}, \tau) - 1 = Y_1(-\infty, \tau) - 1 = 0 \tag{31}$$

$$\left(\frac{\partial \Theta}{\partial \tau} \right)_{\infty, \tau} = \frac{\gamma - 1}{\gamma} \left(\frac{1}{a} - 1 + \Theta_{\infty, \tau} \right) \frac{1}{P} \frac{\mathrm{d}P}{\mathrm{d}\tau} \tag{32}$$

Burning rate for non-QSC model:

$$\dot{r} = \left| \frac{\mathrm{d}\psi_s}{\mathrm{d}\tau} \right| \qquad \text{where} \qquad Y_1(\psi_s, \tau) = 0 \tag{33}$$

Burning rate for QSC model:

$$\dot{r} = \frac{f_R Q_R + \sqrt{f_R^2 Q_R^2 + 4(\Theta_s + Q_c/2) F_1(\Theta_s)}}{2(\Theta_s + Q_c/2)} \tag{34}$$

where

$$F_1 = (\mathcal{A}_c \delta_1 / a \beta_c)(1 - a + a\Theta_s)^2 \exp[-\beta_c / (1 - a + a\Theta_s)]$$

Table 1 Computational grid parameters and accuracy

Quantity	2 MPa	5 MPa
$\Delta\psi$	0.05	0.05
$\psi_\infty - \psi_s$	20	20
$\Delta\tau$	1.13×10^{-3}	1.13×10^{-3}
Δt, s	9.3×10^{-8}	8.28×10^{-8}
η	1.05	1.05
Number of condensed phase grids	300	300
% Error in $\bar{T}_s$	0.14[a]	0.18
% Error in $\bar{T}_\infty$	0.13	0.14
% Error in $\bar{r}$	1.1	1.2

[a]All of the errors are calculated as percentage deviation from the value obtained using analytical solution for temperature in the condensed phase.

V. Method of Solution

Equations (22–34) form a closed set of coupled initial boundary-value problems, parabolic in time. The species and energy equations, both in gas and condensed phase, are numerically solved using the operator-splitting technique. In this scheme the Crank–Nicholson semi-implicit difference is used for the chemical source terms in Eqs. (22–25). The conduction operation in the condensed phase (represented by second-order term in the condensed phase energy equation) is approximated by the Crank–Nicholson scheme, whereas the diffusion operations in the gas phase are treated by an explicit central difference scheme. At the end of each time step, the position of the interface $x_s(t)$ is relocated such that the condensed phase reactant mass fraction Y_1 is zero at the interface. This can be achieved by a simple linear extrapolation of the solution Y_1 from the grids interior to the interface. It was found that the error introduced by this extrapolation could be quite negligible when sufficiently small-sized grids are taken near the interface. The instantaneous burning rate is then calculated as the speed at which the interface moves, using a finite difference approximation to Eq. (33).

For study of pressure-driven frequency response function, the pressure is forced to fluctuate harmonically with a specified amplitude and frequency about a mean value. The complex quantity $R_p(\nu)$ was extracted by the Fourier transform method. For each specified frequency the time-marching calculations were progressed until the cyclic variations in burning rate became time invariant.

The numerical grids are taken uniform in ψ within the gas phase $[\psi > \psi_s(t)]$. The grid size increases exponentially in ψ within the condensed phase. This is achieved by using uniform grids in a transformed coordinate ζ defined by

$$\zeta = 1 - \frac{\ell n\{[\eta + 1 - (\psi - \psi_s)/\psi_{-\infty}]/[\eta - 1 + (\psi - \psi_s)/\psi_{-\infty}]\}}{\ell n[(\eta + 1)/(\eta - 1)]} \tag{35}$$

where η is a stretching parameter (=1.05) used to control the grid compactness.[32] Typically, about 400 grids in the gas phase and 300 grids in the condensed phase are required to get accurate solutions for the range of parameters considered in this study. For further details of the numerical method, Ref. 13 can be consulted.

In the QSC model the maximum computational error in temperature within the condensed phase and the gas-phase flame temperature is less than 0.2% relative to the exact solution. Table 1 shows the computational grid parameters used and the accuracy of the results obtained for steady burning under two different values of pressure.

VI. Results and Discussion

A. Validation of the Non-QSC Model

Zebrowski and Brewster[17] numerically solved the unsteady species conservation equation in the condensed phase including a distributed reaction term. First, the non-QSC model proposed in Sec. III for the propellant burning and the consequent numerical results thereof were validated by comparing its results with those of Ref. 17. In Ref. 17 a radiation assisted burning with an adiabatic gas phase is examined, and therefore the same problem is considered for

Table 2 Baseline properties of the propellant-N (P-1)

Properties	p, MPa 2.0	p, MPa 5.0	Source
Le	1.0	1.0	Assumption
k_c, W/(m K)	0.2312	0.2831	Eq. (3) of Ref. 23
ρ_c, kg/m^3	1,600	1,600	Ref. 23
c_c, J/(kg K)	1,425	1,453	$[-q_c - q_g + q_R/(\rho_c \bar{\dot{r}})]/(\bar{T}_\infty - T_{-\infty})$
$k_{g,\mathrm{ref}}$, W/(m K)	0.03203	0.03199	Eq. (1) of Ref. 23[a]
$\rho_{g,\mathrm{ref}}$, kg/m^3	19.97	49.91	Assumption
c_g, J/(kg K)	1,425	1,453	$-(q_c + q_g)/(\bar{T}_\infty - T_{-\infty})$
q_c, kJ/kg	−397.67	−489.762	Ref. 23
q_g, kJ/kg	−1255.8	−1297.66	Ref. 23
γ	1.4	1.4	Assumption
$\bar{T}_\infty$, K	1,453	1,523	Ref. 23
$\bar{T}_s$, K	613	673	Ref. 23
$T_{-\infty}$, K	293	293	Ref. 23
A_g, m^3/(kg s)	32,000	137,000	Determined by matching measured $\bar{\dot{r}}$ and $\bar{T}_s$ Ref. 23
E_g, J/mol	37,674	37,674	Determined by matching measured profile of temperature in the gas phase at 2.0 MPa Ref. 23
A_c, 1/s	7.512×10^9	5.458×10^9	Determined by matching measured $\bar{\dot{r}}$ and $\bar{T}_s$ Ref. 23
E_c, J/mol	83,720	83,720	Ref. 23

[a]Calculated at $(\bar{T}_\infty + \bar{T}_s)/2$ using Eq. (1) of Ref. 23 and then used the assumption that $k_g \rho_g$ was independent of temperature at all other temperatures.

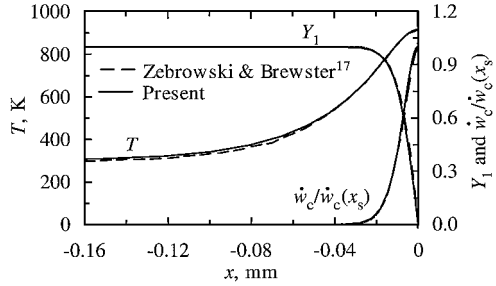

Fig. 2 Steady burning results: comparison of the profiles of temperature, reactant mass fraction, and the chemical source term within the condensed phase.

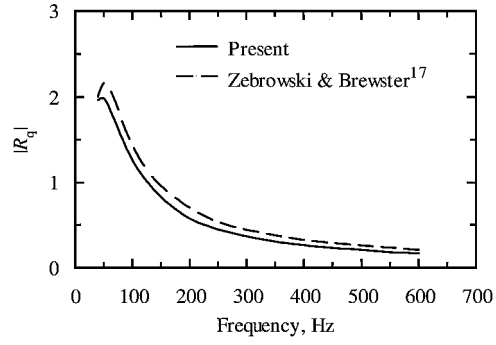

Fig. 3 Radiation-driven dynamic burning results: comparison of the magnitude of the frequency response function $|R_q|$.

the purposes of validation herein. The thermochemical and physical properties of the propellant were also selected as identical to those used in Ref. 17. For the steady burning case the burning rate and the surface temperature obtained from our calculations were 3.11 mm/s and 912.7 K, whereas those reported in Ref. 17 are 3.07 mm/s and 911.5 K, respectively. Figure 2 shows the comparison of steady-state profiles of temperature, mass fraction of reactant species S_1, and normalized reaction rate. Figure 3 shows the comparison of results for the unsteady case, which is presented in terms of the magnitude of R_q. It is seen from these results that the proposed model accurately predicts both the steady and unsteady behavior of radiation-driven propellant burning.

After validating the non-QSC model, calculations were carried out for steady and dynamic pressure-driven burning, including an unsteady gas phase. Hence, these results represent the case of simultaneously relaxing the QSG and QSC assumptions. The unsteady gas-phase modeling with QSC assumption have been validated in a previous work by the authors.[13]

B. Steady Burning Results

Comparison of Predictions with Experimental Data

Numerous measurements of steady burning characteristics of a variety of propellants have been published in the literature. However, a comprehensive set of burning rate and spatial temperature profiles, which is commonly referred to, is the one given by Zenin.[23] In the present study we focus the attention on a single propellant, a typical uncatalyzed DBP, commonly known as "propellant-N." For this propellant Table 2 gives the set of values suggested by Zenin, which form the baseline properties used in the calculations whose results are presented here. This is designated as model propellant "P-1" in the following. A major difficulty in numerical modeling of solid propellant burning is the uncertainty in the global chemical kinetic properties, namely (A_c, E_c, A_g, E_g). Based on experimental measurements of surface temperature and burning rates, Zenin suggests a value of $E_c = 84$ kJ/mol as relatively less uncertain. Hence, this value was taken unchanged herein. As regards the gas-phase properties, a value of $E_g = 54$ kJ/mol at 2 MPa, suggested by Zenin, did not yield a good comparison of predicted temperature profile with his measured profile. Instead, a reduced value of $E_g = 38$ kJ/mol was found to be agreeable (Lengellé et al.[22] suggest a value of $E_g = 21$ kJ/mol). Such a modification in properties was made as follows. First, the value of $E_c = 84$ kJ/mol was taken, and the value of A_c was computed using Eq. (17) to satisfy the measured burning rate and surface temperature. Then, the values of E_g and A_g were found by trial and error so as to match the predicted temperature profile and burning-rate values with those measured experimentally. At a higher pressure of 5 MPa, the same activation energy $E_g = 38$ kJ/mol, but a higher value of A_g was estimated. The respective values of the properties at two different pressures, namely 2 and 5 MPa, are listed in Table 2. In Figs. 4 and 5 the resulting temperature profiles from the QSC and non-QSC model predictions are compared with those measured by Zenin[23] at 2 and 5 MPa, respectively.

Comparison of QSC and Non-QSC Model Results

From Figs. 4 and 5 it is seen that the profiles of temperature in the gas-phase obtained with QSC and non-QSC models are almost identical. A quantitative comparison of the QSC and non-QSC model predictions, at 2 and 5 MPa respectively, has been summarized in

Table 3 Predicted steady burning characteristics; comparison between QSC and non-QSC models

	2 MPa		5 MPa	
Quantity	QSC	Non-QSC	QSC	Non-QSC
$\bar{T}_s$, K	614.6	611.5	675.2	671.6
$\bar{r}$, cm/s	0.347	0.343	0.685	0.676
$k_c\left(\frac{\partial T}{\partial x}\right)_{s-}$, W/cm^2	252	31.5	602	65.2
$\left(k_g\frac{\partial T}{\partial x}\right)_{s+}$, W/cm^2	31	30.7	65	64.7
$\rho_c\bar{r}q_c$, W/cm^2	−221	——	−537	——

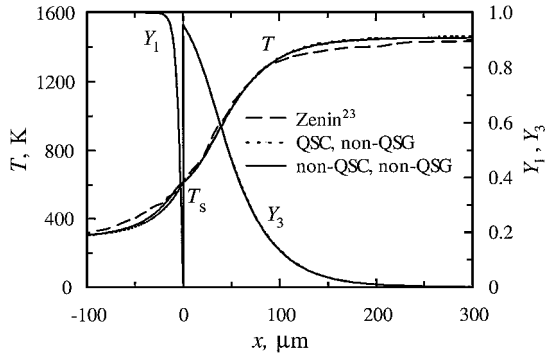

Fig. 4 Steady burning results: comparison of the profiles of temperature and reactant mass fraction for propellant-N (P-1) at $p = 2$ MPa and $T_{-\infty} = 293$ K (with properties listed in Table 2).

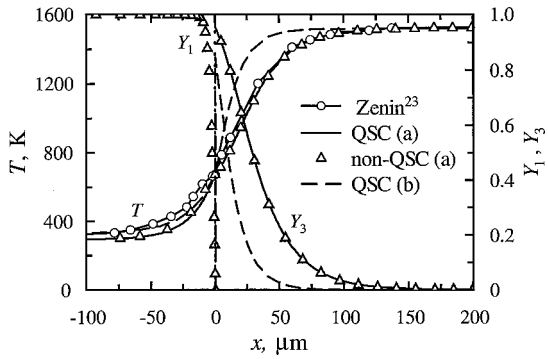

Fig. 5 Steady burning results: comparison of the profiles of temperature and reactant mass fraction for propellant-N at $p = 5$ MPa and $T_{-\infty} = 293$ K: a) Propellant P-1, as in Table 2; and b) propellant P-2, as in Table 2, but with $q_c = -251$ kJ/kg, $q_g = -1453$ kJ/kg, and $q_R = 837$ kJ/(m^2 s).

Table 3. From this, it is seen that the discrepancy in conduction heat flux from the gas phase to the condensed phase is less than 1% at both pressures. However, relaxing the QSC assumption significantly decreased the temperature gradient on the solid side of the interface. A similar behavior was reported in Ref. 17. The error caused in the steady-state surface temperature and burning rate, caused by QSC assumption, is only less than 1 and 2%, respectively. The corresponding values of nondimensional activation energy, $\beta_c = 4.2$ (at 2 MPa) and 3.8 (at 5 MPa), are not considered high in the AEA analysis. Zebrowski and Brewster[17] reported errors of a similar low magnitude for radiation-assisted steady burning without any heat feedback from the gas phase. So, the present results demonstrate that, regardless of the mode of heating of the propellant, the QSC assumption can be valid for steady-state burning even for moderately large values of β_c. However, this finding may not hold well under dynamic burning conditions, as shown subsequently.

Sensitivity of Predictions to Propellant Properties

The measured temperature profiles at high pressures might be underpredicted because of the possible "lag" in the thermocouple technique. Brewster et al.[20] argue that the thermocouple technique introduces a pressure-dependenterror in the gas-phase temperature profile as a result of which the conductive heat flux to the surface from the gas phase is underestimated. Specifically at high pressures this leads to an underestimate in the value of q_g and an overestimate in q_c. It has been suggested that at 5 MPa the actual value of q_c for DBP can be reduced to almost half of that given in Ref. 23. Also, the value of q_g has to be increased appropriately so as to match the flame temperature. These variations in q_c and q_g could change both the steady-state solutions and the frequency response functions. In addition to this, effects of radiation from the secondary flame to the interface can significantly affect the temperature profiles, and hence the relevant terms in the conservation equations have to be adequately modeled.[20] As shown in the next section, the specific set of chosen properties affects also the error in R_p caused by QSC assumption qualitatively as well as quantitatively.

Based on the preceding arguments, an alternative set of properties was selected [$q_c = -251$ kJ/kg, $q_R = 837$ kJ/(m^2 s), $q_g = -1453$ kJ/kg] at 5 MPa. All other properties were same as that given in Table 2, except for A_g, which was chosen to obtain a surface temperature of 673 K. The resulting steady-state temperature profile is also shown in Fig. 5. As expected, the temperatures were uniformly higher than the measured values in the gas phase, and the reaction zone moved toward the interface. These calculations demonstrate that the set of thermokinetic properties chosen for the propellants is crucial, and the resulting steady burning solution depends significantly on these. Such a choice of properties is expected to be even more crucial in the case of dynamic burning, and this aspect is examined in the following section.

C. Dynamic Burning Results

A more important but challenging test for validation of a propellant combustion model is the case of burning under time-varying conditions of pressure and/or radiant heat flux. In the present paper two such dynamic conditions are examined, when the burning is subjected to a pressure that is 1) harmonically fluctuating with a finite, but small amplitude, and 2) rapidly decreasing in time. First, the predicted pressure-driven response function is compared with experimental data, and then the dependence of predicted results on the propellant properties is examined. Subsequently, the effect of introducing unsteadiness in the condensed phase degradation layer (i.e., non-QSC model) is studied.

Comparison of Predicted R_p with Experimental Data

The complex quantity, response function R_p, characterizes the dynamic burning behavior when the pressure fluctuates harmonically around a steady mean value. The commonly used reference experimental data for evaluating theoretical models are those obtained from the T-burner measurements by Horton and Price[33] and Ibiricu.[21] Recently, while reviewing the large body of experimental data on response functions, Brewster[4] concluded that "the original NWC data remains as perhaps the best available for comparison for $|R_p|$, in spite of relatively large uncertainties in the data." Horton and Price[33] studied the JPN propellant, whereas Ibiricu[21] studied many propellants, including JPN. Horton and Price[23] measured the acoustic admittance over frequencies ranging from 500 to 4000 Hz at four mean pressures: 1.4, 2.8, 5.6, and 11.2 MPa, respectively. Ibiricu[21] has given the real part of R_p over a wider range of frequencies, 500–10,000 Hz, at the same mean pressures. In his report Ibiricu[21] observed that these data are scattered, with an uncertainty no better than ±10% in the high-frequency region, while the uncertainty is ±15% or higher at low frequencies. Nevertheless, these data have been used previously for quantitative comparison of theoretical results.[4,20] Therefore, we selected the data reported by Ibiricu[21] for the purposes of comparison with our model predictions. A harmonic fluctuation with an amplitude 1% of the mean pressure (of 5 MPa) was considered, and model predictions of R_p were obtained for different sets of propellant properties, starting from the baseline properties of Table 2.

In Fig. 6 magnitude of the response function measured by Ibiricu[21] for three different propellants, namely, N4, N5, and JPN at 5 MPa, is

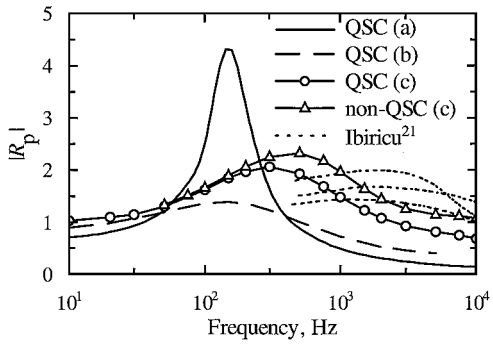

Fig. 6 Pressure-driven dynamic burning results: comparison with experimental measurements of $|R_p|$: a) Propellant P-1, as in Table 2; b) propellant P-2, as in Table 2, but with $q_c = -251$ kJ/kg, $q_g = -1453$ kJ/kg, and $q_R = 837$ kJ/(m^2 s); c) propellant P-3, as in Table 2, but with $q_c = -251$ kJ/kg, $q_g = -1453$ kJ/kg, $q_R = 837$ kJ/(m^2 s), and $E_c = 168$ kJ/mol.

shown. The QSC- model prediction, corresponding to the properties of the propellant P-1 (see Table 2) is also shown on the same plot. Although the measured R_p for different propellants appear to fall within a certain band on the ordinate, the predicted $|R_p|$ using the baseline properties is found to be nowhere near these.

The possible cause for this rather large discrepancy in $|R_p|$ was further investigated. The four basic properties that are known to affect the response function to a first order are E_c, E_g, q_c, and q_g. First, keeping the values of (E_c, E_g) at their baseline levels the values of (q_c, q_g) were altered to those suggested by our steady burning results. Also plotted in Fig. 6 is the response function for this set of properties [$q_c = -251$ kJ/kg, $q_g = -1453$ kJ/kg, and $q_R = 837$ kJ/(m^2 s), designated as propellant "P-2"]. It is seen that the $|R_p|$ for the model propellant P-2 decreased at frequencies below 500 Hz while it increased at frequencies above that in comparison to the predicted values for model propellant P-1. However, the predicted resonant frequency remained unaltered. Any further reduction in q_c was found to have no significant influence on the response function.

Therefore, the attention was next focused on the value of E_c. Apart from the uncertainty in the values of heats of reaction as discussed earlier, there is disagreement over the actual value of overall E_c. A value of approximately $E_c = 84$ kJ/mol was recommended by Zenin[23] based on measurements of steady burning rate and surface temperature. However, as observed by Zenin,[23] the condensed-phase kinetics are dominated by two sets of reactions: those with $E_c = 88$ and 201 kJ/mol. In regions where $T < 523$ K, the former reactions are faster, whereas in regions where $T > 523$ K the latter are faster. In a recent study within the QSHOD framework, Brewster et al.[20] proposed that the comparison of response functions "seem to support" a higher value of $E_c = 168$ kJ/mol. In fact, all of the available experimental results for DBP show a much higher resonant frequency ($\approx$2 kHz). The QSHOD model[6] predicts an increase in the resonant frequency with an increase in E_c. So, we calculated the response function with $E_c = 168$ kJ/mol (designated as propellant "P-3"), and the corresponding result is also shown in Fig. 6. This resulted in a higher resonant frequency of about 300 Hz, which is yet an order less than the experimental values.

All of the preceding calculations were performed within the QSC framework. Next, the response function calculations were carried out using the non-QSC model for the propellants P-1 and P-2. This increased the magnitude of the response function over all of the frequencies (not shown in Fig. 6), but the result was yet quite different from the experimental data. Nevertheless, the non-QSC model result of $|R_p|$ for the propellant P-3 showed a marked improvement in the magnitude of the response function. Also, it shifts the resonant frequency to the right by a factor of two relative to the results of QSC model for the same propellant. Hence, the present calculations with non-QSC model suggest a higher value for the overall activation energy E_c than what has been suggested in Ref. 23.

Other factors could influence the predicted response function. First, most authors (including the present) have used the steady burning measurements of surface temperature and burning rate given by Zenin for propellant N for comparison of R_p of other propellants. This may not be appropriate, and instead a different set of data for JPN, N-4, and N-5 might have to be used because their steady-state burning rates are much higher than that of propellant N. Unfortunately, the actual values of thermokinetic properties (q_c, q_g, E_c, E_g) and temperature profiles are not available in the open literature. Assuming thermophysical properties similar to propellant N, this corresponds to a smaller t_c and, hence, a higher resonant frequency. Second, the decomposition mechanism in the condensed phase might be different for different propellants, and a more detailed reaction mechanism within the condensed phase might be warranted for modeling. Nevertheless, the present study shows that even for higher values of E_c the relaxation of QSC assumption changes both the magnitude of the response function and the resonant frequency significantly.

Comparison of R_p from QSC and Non-QSC Models

The QSC assumption is expected to breakdown at driving frequencies of the order of the characteristic frequency of the condensed-phase reaction zone t_r^{-1}. In this case $t_r^{-1} = 5534$ Hz at 5 MPa (corresponding $E_c = 168$ kJ/mol, $T_s = 673$ K). However, Zebrowski and Brewster[17] found that the QSC model caused a significant error in R_q even at frequencies as low as one-fourth of t_r^{-1}. In the present work such a study was extended to the case of pressure-driven burning. In Fig. 6 the magnitude of R_p increased over the entire range of frequencies considered when the QSC assumption was relaxed. However, the increase was not uniform, and a quantitative variation is not evident directly. Therefore, the quantitative difference between the QSC and non-QSC model predictions in $|R_p|$ was calculated at different driving frequencies.

Shown in Fig. 7 is the variation of error in $|R_p|$ from the QSC model, as a relative percentage of the $|R_p|$ predicted from the non-QSC model. The driving frequency is normalized with respect to $t_r^{-1} = 5534$ Hz. The error caused by QSC assumption is found to increase to significant values at frequencies near the resonant peak, which is about 10 times lower than t_r^{-1}. Then it decreases slightly, but starts to increase again as the frequency approaches the characteristic frequency of the condensed phase reaction zone. The breakdown of QSC model at driving frequencies higher than t_r^{-1} was expected, but large errors near the resonant frequency were not. The frequency response computed for other sets of properties of propellant also showed large errors at lower frequencies (indicated in Fig. 7). Therefore, the present results demonstrate the importance of non-QSC effects at driving frequencies much lower than the expected ones near t_r^{-1}.

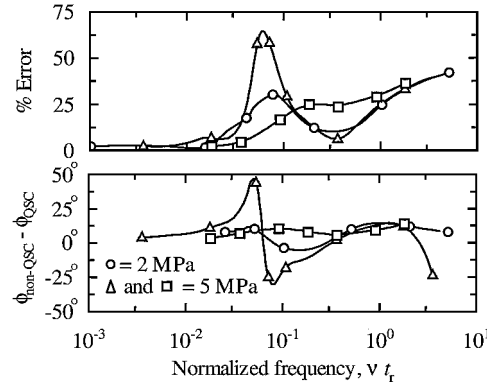

Fig. 7 Pressure-driven dynamic burning results: error caused by QSC assumption in the predicted magnitude $|R_p|$ and phase ϕ. The error in magnitude is defined as $(|R_{p,\text{non-QSC}}| - |R_{p,\text{QSC}}|) \times 100/|R_{p,\text{QSC}}|$. –o– $p = 2$ MPa (propellant P-1, as in Table 2), –△– $p = 5$ MPa (propellant P-1, as in Table 2), –□– $p = 5$ MPa, (propellant P-3, as in Table 2, but with $E_c = 168$ kJ/mol, $q_c = -251$ kJ/kg, $q_g = -1453$ kJ/kg), and $q_R = 837$ kJ/(m^2 s).

An interesting result to be observed here is that the effect of relaxing the QSC assumption on R_p and on R_q is qualitatively different. For radiation-driven burning Zebrowski and Brewster[17] found that relaxing the QSC assumption underpredicts the $|R_q|$ in low-frequency region and does more so near the resonant frequency. On the other hand, the present results for $|R_p|$ show an opposite trend. In radiation-driven burning any fluctuation in the incident radiant flux causes instantaneous fluctuations in the local radiant heat flux at all points interior of the interface. However, in pressure-driven burning any fluctuation in the conduction heat feedback from the gas phase could instantaneously influence only the interface, but takes a finite time to be transported by conduction into the interior locations in the condensed phase. So, the influence of the two different driving forces, external radiation and pressure, on the response of the chemical reaction zone is qualitatively different. This could lead to the observed qualitative difference in the effect of relaxing the QSC assumption respectively on R_q and R_p. This result emphasizes the importance of 1) proper modeling of the unsteadiness of the gas phase and 2) a detailed study of the relation between R_p and R_q. The second aspect is significant in view of the increasing interest in using the parameters calculated from R_q measurements to compute R_p (Ref. 19).

D. Extinction by Rapid Depressurization

As discussed in Sec. VI.C, the error caused by QSC assumption could be large even at low frequencies, when the surface temperature fluctuates with large amplitudes. Therefore, herein the effect of relaxing the QSC assumption on the rapid depressurization transients is examined.

The following procedure is used for simulating a rapid depressurization transient. First, keeping the pressure at a high, but constant value (p_i), a steady-state solution is obtained. From this initial state the pressure is decreased to a prescribed lower value (p_f). The corresponding temporal variation of pressure is assigned an exponential decay in the form

$$p(t) = p_i - (p_i - p_f)[1 - \exp(\alpha t)] \tag{36}$$

for $\alpha < 0$. Unsteady calculations are performed to obtain the instantaneous burning rate evolution $\dot{r}(t)$ in time. The effect of QSC and non-QSC models on the evolution of $\dot{r}(t)$ is studied for different parametric values of initial depressurization rates $(p_i - p_f)\alpha$. The results presented herein pertain to $p_i = 5$ MPa and $p_f = 0.5$ MPa for the propellant P-1.

Certain remarks concerning the thermochemical properties of the propellant are in order. Because this simulation involves a large change in pressure, proper variation in the thermokinetic properties (A_c, A_g, q_c, q_g) as a function of the instantaneous pressure must be taken into account. The variation of these properties is taken so as to satisfy the steady burning data[23,34] at four intermediate pressures, namely, 5, 2, 1, and 0.5 MPa. Thermal conductivities and specific heats (k_c, k_g, c_c, c_g) were kept constant in these simulations. However, the sensitivity of transient burning characteristics during depressurization to variation of these properties remains to be examined.

In contrast to the R_p calculations presented in the preceding section, the pressure transient calculations were not intended for any quantitative comparison with experimental results at this stage. Variations in the physical and chemical structure of the reaction zone in the condensed phase and the gas phase are more complex than modeled herein. Specifically, the presence of a prominent dark zone at pressures below 5 MPa could significantly alter the results. Nevertheless, certain principal features of the rapid depressurization effect on propellant burning could be demonstrated with the simple kinetic models used here. For example, flame luminosity and gas-phase temperature measurements during depressurization experiments reveal certain salient features.[25–28] Two important such features are as follows: 1) a critical initial depressurization rate below which burning continues and above which the extinction occurs and 2) reignition following extinction when the depressurization is not too fast and/or final pressure is not too low. In the present work first these features are reproduced, and then the effect of relaxing the QSC assumption on these is examined.

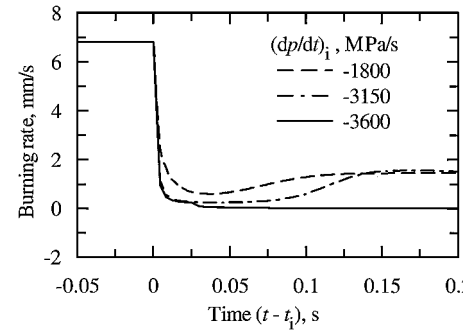

Fig. 8 Computed evolution of the burning rate during a fast depressurization transient: results of the QSC model.

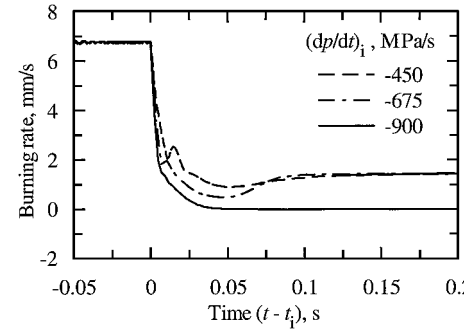

Fig. 9 Computed evolution of the burning rate during a fast depressurization transient: results of the non-QSC model.

Figure 8 shows the evolution of burning rate obtained using QSC model for three different initial rates of depressurization. For values of $(dp/dt)_i = -1800$ and -3150 MPa/s, burning rate initially decreased, but however recovered slowly and finally reached the steady state corresponding to $p_f = 0.5$ MPa. In the former case the lowest value of burning rate ever was only about 50% of the final value, whereas in the second case it was as small as about 13% and remained like so over a period as long as about 70 ms. The flame temperature also varied in a similar manner. Considering that about 62% of the pressure drop occurred within a period of 1.7 ms, the second case can be taken to represent a limiting case, which leads to combustion recovery. On the other hand, when the initial pressure decay rate was increased to $(dp/dt)_i = -3600$ MPa/s the burning rate decreased to very small values and did not recover even after 225 ms. Hence, the third case exhibited extinction, which fails to reignite. Extinction was observed for any value of $(dp/dt)_i$ faster than this critical value. Therefore, the critical depressurization rate can be taken as between 3150 and 3600 MPa/s.

Similar computations were performed with the non-QSC model, and the results are shown in Fig. 9. In this case the evolution of the burning rate was qualitatively the same as that of the QSC model except for the slight deviation from the monotonic decrease in the initial stage in some cases. However, for other parametric ranges non-QSC model results can feature, besides larger sensitivity to a rapid pressure drop, a more prominent deviation from monotonic rate decrease, ignition and possible oscillatory behavior. Whether such results can be obtained will form important issues of future work. In the present case relaxing the QSC assumption decreased the critical depressurization rate by about a factor of four. This implies that the non-QSC model is more sensitive to rapid pressure variation and confirms our observations in Sec. VI.C with respect to dynamic stability and R_p.

VII. Conclusions

For steady burning the QSC assumption based on high activation energy asymptotics is acceptable for realistic values of condensed phase activation energy. However, for unsteady pressure-driven burning the error introduced by the QSC assumption is much larger and occurs even at low frequencies, for similar values of activation energy. Hence, relaxing of both QSC and QSG assumptions are equally important to compute the unsteady burning characteristics of solid propellants. A quantitative comparison of the predicted response function (magnitude) with experimental data has been attempted for double base propellants. This seems to suggest that the value of overall activation energy of reactions in the condensed phase is probably higher than that suggested by Zenin.

For pressure-driven burning relaxing the QSC assumption results in an increase in the response function magnitude $|R_p|$. However, this is qualitatively different from the reported behavior of radiation-driven response function magnitude $|R_q|$. Results of unsteady simulations of burning under a rapid depressurization transient exhibit salient features of combustion recovery and extinction observed in experiments. The predicted critical depressurization rate markedly decreased (by a factor of four) when the QSC assumption was relaxed.

Acknowledgment

This research was funded by the ISRO-IISc Space Technology Cell.

References

[1]Price, E. W., "Solid Rocket Combustion Instability—An American Historical Account," *Nonsteady Burning and Combustion Stability of Solid Propellants*, edited by L. De Luca, E. W. Price, and M. Summerfield, Vol. 143, Progress in Astronautics and Aeronautics, AIAA, Washington, DC, 1992, pp. 1–16.

[2]Barrère, M., "Introduction to Nonsteady Burning and Combustion Stability," *Nonsteady Burning and Combustion Stability of Solid Propellants*, edited by L. De Luca, E. W. Price, and M. Summerfield, Vol. 143, Progress in Astronautics and Aeronautics, AIAA, Washington, DC, 1992, pp. 17–58.

[3]Mathes, H. B., "Applications of Combustion-Stability Technology to Solid-Propellant Rocket Motors," *Nonsteady Burning and Combustion Stability of Solid Propellants*, edited by L. De Luca, E. W. Price, and M. Summerfield, Vol. 143, Progress in Astronautics and Aeronautics, AIAA, Washington, DC, 1992, pp. 781–804.

[4]Brewster, M. Q., "Solid Propellant Combustion Response: Quasi-Steady (QSHOD) Theory Development and Validation," *Solid Propellant Chemistry, Combustion, and Motor Interior Ballistics*, edited by V. Yang, T. B. Brill, and W. Ren, Vol. 186, Progress in Astronautics and Aeronautics, AIAA, Reston, VA, 2000, pp. 607–638.

[5]Kuo, K. K., Gore, J. P., and Summerfield, M., "Transient Burning of Solid Propellants," *Fundamentals of Solid-Propellant Combustion*, edited by K. K. Kuo and M. Summerfield, Vol. 90, Progress in Astronautics and Aeronautics, AIAA, New York, 1984, pp. 599–659.

[6]Denison, M. R., and Baum, E., "A Simplified Model of Unstable Burning in Solid Propellants," *ARS Journal*, Vol. 31, No. 8, 1961, pp. 1112–1122.

[7]Novozhilov, B. V., "Theory of Nonsteady Burning and Combustion Stability of Solid Propellants by the Zel'dovich-Novozhilov Method," *Nonsteady Burning and Combustion Stability of Solid Propellants*, edited by L. De Luca, E. W. Price, and M. Summerfield, Vol. 143, Progress in Astronautics and Aeronautics, AIAA, Washington, DC, 1992, pp. 601–641.

[8]De Luca, L., Di Silvestro, R., and Cozzi, F., "Intrinsic Combustion Instability of Solid Energetic Materials," *Journal of Propulsion and Power*, Vol. 11, No. 4, 1995, pp. 804–815.

[9]T'ien, J. S., "Oscillatory Burning of Solid Propellants Including Gas Phase Time Lag," *Combustion Science and Technology*, Vol. 5, No. 2, 1972, pp. 47–54.

[10]Novozhilov, B. V., "The Effect of a Gas-Phase Thermal Lag on Combustion Stability of Volatile Condensed Systems," *Soviet Journal of Chemical Physics*, Vol. 7, No. 3, 1990, pp. 616–632.

[11]Clavin, P., and Lazimi, D., "Theoretical Analysis of Oscillatory Burning of Homogeneous Solid Propellant Including Non-Steady Gas Phase Effects," *Combustion Science and Technology*, Vol. 83, No. 1–3, 1992, pp. 1–32.

[12]Novozhilov, B. V., "Acoustic Admittance of the Surface of Burning Condensed Matter," *Soviet Journal of Chemical Physics*, Vol. 10, No. 11, 1993, pp. 2363–2384.

[13]Anil Kumar, K. R., and Lakshmisha, K. N., "Nonlinear Intrinsic Instability of Solid Propellant Combustion Including Gas-Phase Thermal Inertia," *Combustion Science and Technology*, Vol. 158, No. 1–6, 2000, pp. 135–166.

[14]Louwers, J., and Gadiot, G. M. H. J. L., "Model for Nonlinear Transient Burning of Hydrazinium Nitroformate," *Journal of Propulsion and Power*, Vol. 15, No. 6, 1999, pp. 778–782.

[15]Lengellé, G., "Thermal Degradation Kinetics and Surface Pyrolysis of Vinyl Polymers," *AIAA Journal*, Vol. 8, No. 11, 1970, pp. 1989–1996.

[16]Ibiricu, M. W., and Williams, F. A., "Influence of Externally Applied Thermal Radiation on the Burning Rates of Homogeneous Solid Propellants," *Combustion and Flame*, Vol. 24, Feb.–June 1975, pp. 185–198.

[17]Zebrowski, M. A., and Brewster, M. Q., "Theory of Unsteady Combustion of Solids: Investigation of Quasisteady Assumption," *Journal of Propulsion and Power*, Vol. 12, No. 3, 1996, pp. 564–573.

[18]De Luca, L., and Galfetti, L., "Combustion Modeling and Stability of Double-Base Solid Rocket Propellants," *Modern Research Topics in Aerospace Propulsion*, Springer-Verlag, New York, 1991, pp. 109–134.

[19]Brewster, Q., and Son, S. F., "Quasi-Steady Combustion Modeling of Homogeneous Solid Propellants," *Combustion and Flame*, Vol. 103, No. 1/2, 1995, pp. 11–26.

[20]Brewster, M. Q., Ward, M. J., and Son, S. F., "Simplified Combustion Modeling of Double Base Propellant: Gas Phase Chain Reaction vs. Thermal Decomposition," *Combustion Science and Technology*, Vol. 154, 2000, pp. 1–30.

[21]Ibiricu, M. W., "Experimental Studies on the Oscillatory Combustion of Solid Propellants," Naval Weapons Center, NWC TP 4393, China Lake, California, March 1969.

[22]Lengellé, G., Bizot, A., Duterque, J., and Trubert, J. F., "Steady-State Burning of Homogeneous Propellants," *Fundamentals of Solid-Propellant Combustion*, edited by K. K. Kuo and M. Summerfield, Vol. 90, Progress in Astronautics and Aeronautics, AIAA, New York, 1984, pp. 361–405.

[23]Zenin, A. A., "Thermophysics of Stable Combustion Waves of Solid Propellants," *Nonsteady Burning and Combustion Stability of Solid Propellants*, edited by L. De Luca, E. W. Price, and M. Summerfield, Vol. 143, Progress in Astronautics and Aeronautics, AIAA, Washington, DC, 1992, pp. 197–231.

[24]DeLuca, L., "Extinction Theories and Experiments," *Fundamentals of Solid Propellant Combustion*, edited by K. K. Kuo and M. Summerfield, Vol. 90, Progress in Astronautics and Aeronautics, AIAA, New York, 1984, pp. 661–732.

[25]Ciepluch, C. C., "Effects of Rapid Pressure Decay on Solid Propellant Combustion," *ARS Journal*, Vol. 31, No. 11, 1961, pp. 1584–1586.

[26]Ciepluch, C. C., "Effect of Composition on Combustion of Solid Propellants During a Rapid Pressure Decrease," NASA TN D-1559, Dec. 1962.

[27]Ciepluch, C. C., "Spontaneous Reignition of Previously Extinguished Solid Propellants," NASA TN D-2167, March 1964.

[28]Zemskikh, V. I., Istratov, A. G., Leipunskii, O. I., and Marshakov, V. N., "Three Characteristic Ballistic Powder Combustion Modes with a Pressure Drop," *Combustion Explosion and Shock Waves*, Vol. 13, No. 1, 1977, pp. 11–15.

[29]T'ien, J. S., "A Theoretical Criterion for Dynamic Extinction of Solid Propellants by Fast Depressurization," *Combustion Science and Technology*, Vol. 9, 1974, pp. 37–39.

[30]Cozzi, F., De Luca, L. T., and Novozhilov, B. V., "Linear Stability and Pressure-Driven Response Function of Solid Propellants with Phase Transition," *Journal of Propulsion and Power*, Vol. 15, No. 6, 1999, pp. 806–815.

[31]Williams, F. A., "Quasi-Steady Gas-Phase Flame Theory in Unsteady Burning of a Homogeneous Solid Propellant," *AIAA Journal*, Vol. 11, No. 9, 1973, pp. 1328–1330.

[32]Son, S. F., "The Unsteady Combustion of Radiant Heat Flux Driven Energetic Solids," Ph.D. Dissertation, Mechanical Engineering in the Graduate College, Univ. of Illinois at Urbana-Champaign, IL, 1994.

[33]Horton, M. D., and Price, E. W., "Dynamic Characteristics of Solid Propellant Combustion," *Proceedings of Combustion Institute*, Academic Press, New York and London, Vol. 9, 1963, pp. 303–310.

[34]Kovalskii, A. A., Konev, E. V., and Krasilnikov, B. V., "Combustion of Nitroglycerine Powder," *Combustion Explosion and Shock Waves*, Vol. 3, No. 4, 1967, pp. 335–339.